Propagation along a Human Body Surface in WBAN

Remarks of Desirable Antenna Characteristics

Markus Berg, Tommi Tuovinen
Centre for Wireless Communications, Department of Communications Engineering
University of Oulu, Finland
Oulu, Finland
{firstname.surname}@ee.oulu.fi

***Abstract*—High on-body channel path gain and the low radio frequency power consumption of a sensor node are of increasing interest for body area network applications. The present paper investigates the desired characteristics of an efficient antenna for such networks and on-body propagation along various body surface phantoms.**

Keywords—body surface waves; on-body antenna; polarization

I. INTRODUCTION

The increased development work and research of wearable technologies have yielded to the compact size of components and miniaturized antenna solutions providing more comfortable user experience at the end. The significant milestone of the recent development has been the publication of the international WBAN standard IEEE802.15.6 [1] in 2012. Based on the literature, the great boost of wearable antenna and propagation research for WBANs was started in the middle of the last decade [2]-[7]. The generality of the antennas for the use close to a human body have been planar [8]-[11] for the allocated on-body frequencies around 900 MHz, 2400 MHz [12] or FCC UWB regulations [13], introduced in 802.15.6 [1].

Despite the recent advances, the planar antenna structures intended to on-body communications often suffer from the unnecessary high channel path loss. This is due to the antenna polarization and radiation pattern in the tangential direction with a human body surface. Depending on the position and orientation of the antennas on-body, the achievable path gain is observed to face variations. The effect of the antenna alignment resulting in the variation of polarization has the significantly greater impact on the path loss in the case of channel paths around a body, as demonstrated in [14]-[15], in comparison with the flat surface. In order to achieve the wave propagation along the body and mitigating the impact of the antenna alignment, the surface waves of a body are crucial to excite by generating the normal polarization with the body surface. This enables the better path gain on a link; indirectly the power consumption of a sensor node is lower or the amount of nodes on a body can possibly be reduced due to the better propagation.

Research is supported in part by the research projects "Reconfigurable Antennas and Over-the-Air Test for Cognitive Radios" and "Enabling Wireless Healthcare Systems (EWiHS)" in Centre for Wireless Communications at University of Oulu and Infotech Oulu Doctoral Program, Finland. Nokia foundation is appreciated for the financial support of the doctoral degree research of the second author.

The research problem returns to the creeping wave theory (CWT) [16]. Recently, this fundamental question has been studied by examining the miniaturized antenna structures with the desired patterns in addition to the normal polarization to the body surface [17]-[18]. In this paper, the features of efficient on-body antennas with different polarizations are summarised in addition to the demonstration of the propagation along body tissue phantoms at 2.45 GHz. Simulations are carried out by using Computer Simulation Technology (CST) software with finite integration technique.

II. EXPERIMENTAL SETUP

In this paper, three various types of antennas, as shown in Fig. 1, are studied to compare the on-body channel path gain performance. The discone and dipole are originally published in [14]. The discone includes the cone with the height of 34.8 mm and the radius of 3 mm at the end while a disc of the structure is of the height of 1 mm and the radius of 5 mm. The dipole consists of direct copper strips of the size of 22.5 x 0.2 mm^2, and the feed gap of 0.5 mm. A substrate below the dipole of the size 49.5 x 4.2 mm^2 is made of a 0.8 mm thick FR4 with ε_r = 4.3. The planar inverted-F antenna (PIFA), presented for the first time in [15], has a ground plane of the size of 25 x 35 mm^2 (thickness = 0.5 mm) and the substrates are made of FR4, while a radiating element in the substrate is with the size of 8.0 x 12.4 mm^2. More details are available in the original papers.

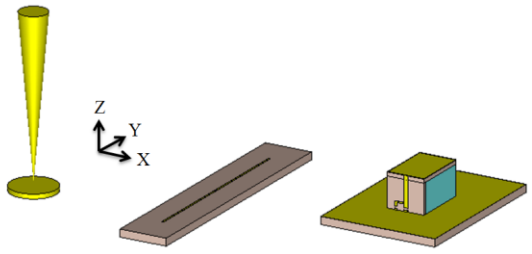

(a) (b) (c)

Figure 1. Studied antenna configurations: discone, planar dipole and PIFA.

In addition to the channel in free space, three various tissue phantoms are used for the examinations of the on-body channels. A planar rectangular phantom, in Fig. 2 (top) is of the size of 80 (x) x 50 (y) x 5 (z) cm^3. The size of the corrugated surface phantom in Fig. 2 (middle) is equal with the planar phantom. The height of a single fold in the z-direction is 5 cm while the width in the x-direction is approx. 10 cm.

MOBIHEALTH 2014, November 03-05, Athens, Greece

DOI 10.4108/icst.mobihealth.2014.257362

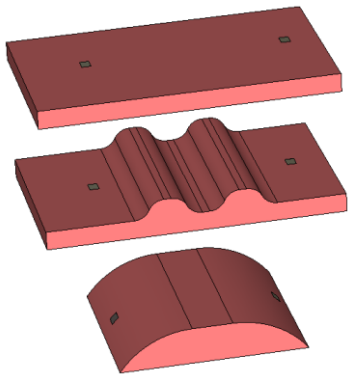

Figure 2. Body tissue phantoms and antenna positions to study.

In Fig. 2 (bottom), a curved phantom is of the size of 50 (x) x 50 (y) x 5 (z) cm^3 with the blending radius of 2.5 cm. The properties of tissues are determined by relative permittivity ε_r = 38.063 and conductivity σ = 1.4407 S/m.

III. Results

The discrepancies of path loss between parallel and perpendicular alignments (as defined in [14]) for the planar dipole on the planar phantom are shown in Figs. 3(a)-(b). Being determined by the alignment, the performance of the dipole in Fig. 1 varies from -31.7 to -52.5 dB and from -38.5 to -65.5 dB between the studied alignments and paths. Due to the feasible on-body characteristics, the path gain of the discone, visible in Fig. 3(c) remains constant depending on the alignment on the tissue phantom. The path gain of the discone is better than -31.8 dB for the paths smaller than 50 cm. The nearly omnidirectional radiation pattern of the PIFA in the xy-plane in the vicinity of the planar phantom is the reason why the performance variation between the studied alignments is smaller than 0.4 dB for the paths through the range of 10 – 50 cm.

Fig. 4 compares the electric field distributions above the planar phantom and in free space. As visible, the distributions of the planar dipole become a directive to the upper hemisphere above the phantom (a)-(b), by mitigating the components propagating in the tangential direction with respect to the phantom surface. Instead, for the discone (Fig. 4 (c)), the distributions of the components at the xy-plane resemble the operation in free space, and the performance is not seen significantly vary between these propagation environments, as

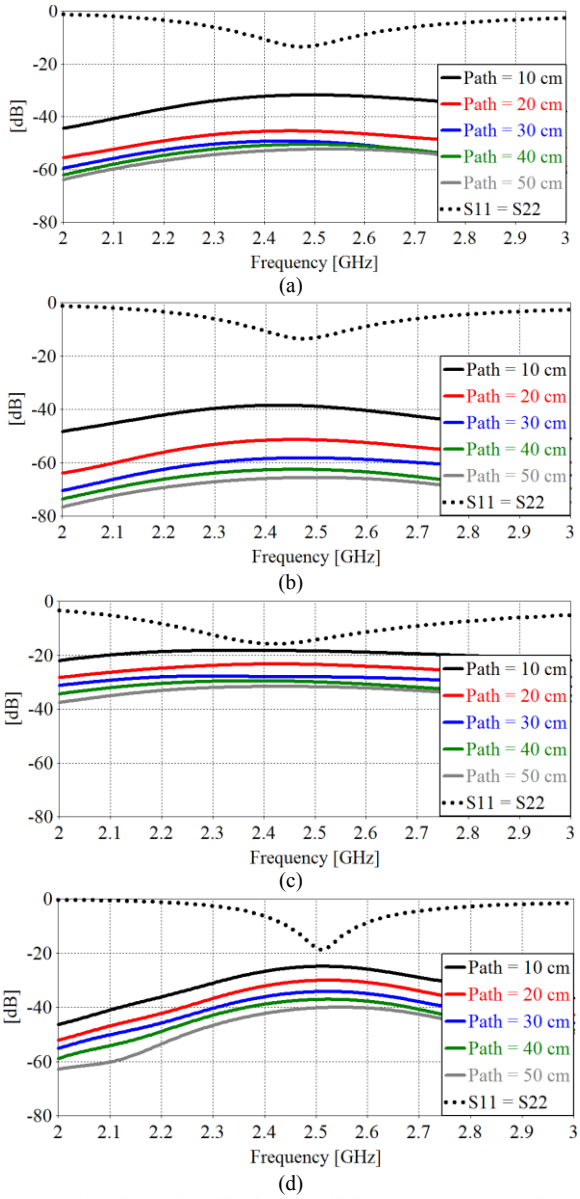

Figure 3. Path gain and reflection coefficient on a rectangular tissue-equilevant phantom for antenna configurations to cover the Bluetooth spectrum: (a) dipole - parallel alignment, (b) dipole – perpendicular aligment, (c) discone – both alignments, and (d) PIFA – both alignments. To allow a fair comparison in terms of matching, the height of the dipole and discone above the phantom is $\lambda_0/4$, whereas a ground of the PIFA is on contact the phantom.

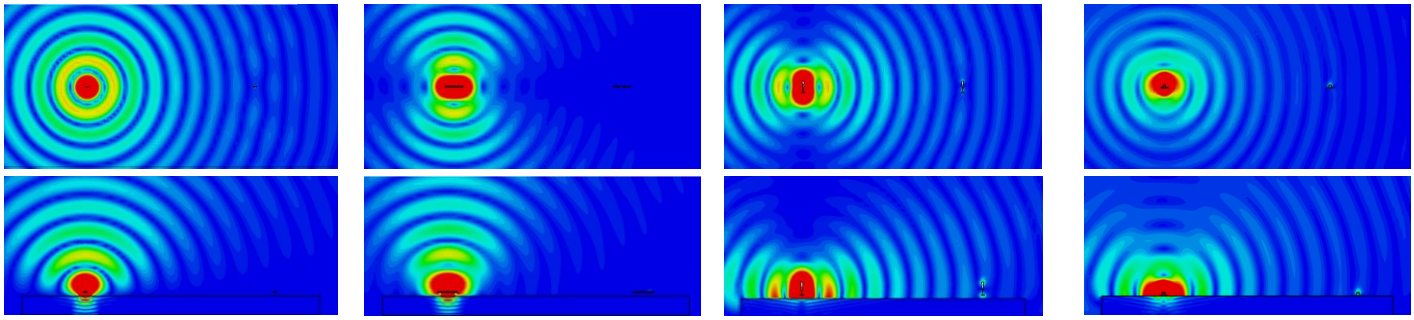

Figure 4. E-field distributions [V/m] at the xz-plane in free space (above) and on contact the planar phantom (below) for the path of 50 cm: (a) dipole - parallel alignment, (b) dipole - perpendicular alignment, (c) discone – both, and (d) PIFA – parallel alignment.

TABLE I. CHANNEL PATH GAIN (PATH OF 50 CM) AT 2.45 GHZ FOR VARIOUS PHANTOM MODELS IN COMPARISON WITH FREE SPACE

Phantom model	**Antenna configuration and alignment**				
	Dipole - parallel	***Dipole - perpendicular***	***Discone - both***	***PIFA - parallel***	***PIFA - perpendicular***
In free space	-31.4 dB	-58.8 dB	-30.7 dB	-43.4 dB	-44.3 dB
Planar phantom	-55.7 dB	-60.1 dB	-32.5 dB	-39.8 dB	-39.2 dB
Corrugated phantom	-60.0 dB	-64.3 dB	-41.5 dB	-47.9 dB	-47.1 dB
Curved phantom	-68.9 dB	-81.6 dB	-40.7 dB	-48.8 dB	-49.4 dB

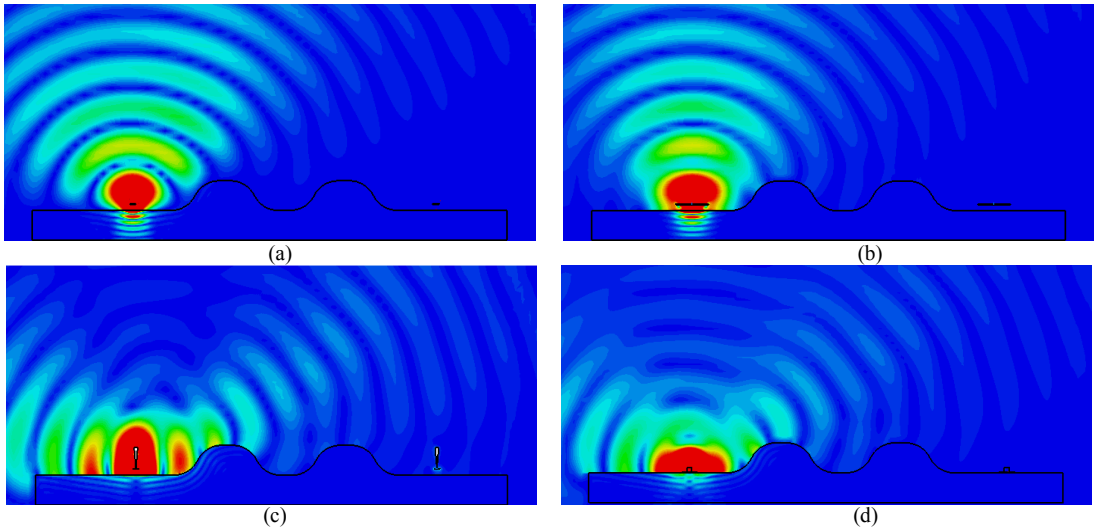

(a) (b) (c) (d)

Figure 5. E-field distributions [V/m] at the *xz*-plane on the crumbled phantom (path of 50 cm) for studied antenna configurations: (a) dipole - parallel alignment, (b) dipole – perpendicular alignment, (c) discone - both alignments, and (d) planar inverted F-antenna (or patch) – parallel alignment

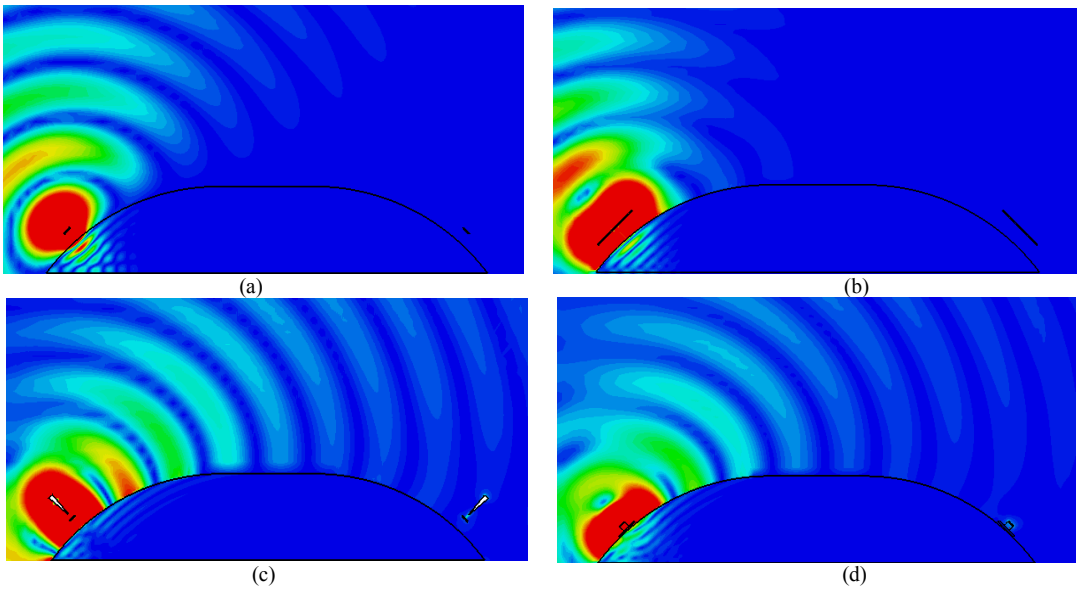

(a) (b) (c) (d)

Figure 6. E-field distributions [V/m] at the *xz*-plane on the curved phantom (path of 50 cm) for studied antenna configurations: (a) dipole - parallel alignment, (b) dipole – perpendicular alignment, (c) discone - both alignments, and (d) planar inverted F-antenna (or patch) – parallel alignment

visible also in the results of Table 1 in terms of path gain. For the on-ground PIFA, the impact of the phantom on the pattern shape modification is favourable. As seen in Table 1, in addition to the plots in Fig. 4(d), the *E*-field distribution of the PIFA in the proximity of the body resembles the discone.

On-body propagation along the corrugated and curved phantoms is depicted in Figs. 5-6. In comparison with the planar phantom, the impact of the folds on path gain is from -4.2 to -4.3 dB for the alignments of the planar dipole. For the discone and PIFA, with the omnidirectional properties at the *xy*-plane, the first fold in Figs. 5(c)-(d) is observed to act as reflector resulting in the change of the field distribution. In addition, a proportion of the field propagates over the folds as seen in the pictures. The corresponding decrease in path gain is 9 dB for discone and 7.9 – 8.1 dB for the PIFA. The small decrease in the case of the dipole is supposedly due to the directive *E*-field distribution above the phantom.

Figs. 6(a)-(d) demonstrate the impact of the normal polarization (in the case of the discone and PIFA) to forward the *E*-field along the curvature of two media interfaces. In comparison with the free space, as shown in Table 1, the dipole link has an over 30 dB lower path gain against the 10 dB decrease for the two-discone link path gain. At the same time, the decrease in path gain with two PIFAs is only 5 dB. However, the path gain level for PIFAs is several decibels lower than that of discone. These indicate the favourable influence of the phantom on the on-body radiation parameters of the PIFA.

The influence of the normal polarization is beneficial in order to maximise the link budget in addition to minimize the power consumption of a sensor node. Especially, in the case a body of the user (a human being or an animal) is large, the impact of polarization is crucial to optimise for high performance.

At the end, the beneficial features of on-body antennas are summarized as follows. The high-efficient on-body antenna has

- omnidirectional pattern in the tangential direction, and
- the normal polarization with the body surface.

To achieve these properties will then

- maximize coupling between two antennas on-body,
- launch body surface waves, i.e., creeping waves, and
- minimize off-body radiation.

IV. CONCLUSIONS

In this paper, we have demonstrated the effect of the type and orientation (that are the polarization and radiation pattern) on the path gain between two on-body antennas. Simulations were realized for three various body tissue phantoms; planar, corrugated and curved. It was observed that the vertical discone antenna showed the highest path gain for each propagation environment because of the vertical polarization and omnidirectional radiation pattern it has. Respectively, the on-ground PIFA showed approximately 6 dB lower path gain with all the phantoms. The planar dipole had the lowest gain because of the non-optimal pattern and polarization for the on-body usage.

It is concluded that both antenna polarization and radiation pattern have a significant effect on on-body propagation performance. In order to obtain high path gain one must design an antenna structure, which has both the maximum gain in the tangential direction of a body and the vertical polarization in order to launch body's creeping waves. For practical antennas, this is a challenge because of the limited dimension in the vertical direction to the body.

REFERENCES

[1] IEEE standard for local and metropolitan area networks, IEEE 802.15.6-2012 – Part 15.6: wireless body area networks, 2012

[2] P. S. Hall, Y. Hao, Y. I. Nechayev, A. Alomainy, C. C. Constantinou, C. Parini, M. R. Kamarudin, T. Z. Salim, D. T. M. Hee, R. Dubrovka, A. S. Owadally, W. Song, A. Serra, P. Nepa, M. Gallo and M. Bozzetti, "Antennas and Propagation for On-Body Communication Systems," *IEEE Antennas Propag. Magaz.*, vol. 49, no. 3, pp. 41-58, Jun. 2007.

[3] T. S. P. See and Z. N. Chen, "Experimental characterization of UWB antennas for on-body communications," *IEEE Trans. Antennas Propag.*, vol. 57, no. 4, pp. 866-874, Apr. 2004.

[4] A. Alomainy, Y. Hao, C. G. Parini and P. S. Hall, "Comparison between two different antennas for UWB on-body propagation measurements," *IEEE Antennas Wirel. Propag. Lett.*, vol. 4, pp. 31-31, 2005.

[5] Z. N. Chen, M. J. Ammann, X. Qing, X. H. Wu, T. S. P. See and A. Cai, "Planar antennas," *IEEE Microw. Magaz.*, pp. 63-73, Dec. 2006.

[6] A. Alomainy, Y. Hao and F. Pasveer, "Numerical and experimental evaluation of a compact sensor antenna for healthcare devices," *IEEE Trans. Biomed. Circuits Syst.*, vol. 1, no. 4, pp. 242-249, Dec. 2007.

[7] Z. N. Chen, *Antennas for Portable Devices*, England: John Wiley & Sons Ltd, 2007.

[8] G. A. Conway and W. G. Scanlon, "Antennas for over-body-surface communication at 2.45 GHz", *IEEE Trans. Antennas Propag.*, vol. 57, no. 4, pp. 844-855, Apr. 2009.

[9] T. Tuovinen, M. Berg, K. Yekeh Yazdandoost and J. Iinatti, "Ultra wideband loop antenna on contact with human body tissues," *IET Microw. Antennas Propag.*, vol. 7, no. 7, pp. 588-596, May 2013.

[10] P. J. Soh, G. A. E. Vandenbosch, S. L. Ooi and N. H. M. Rais, "Design of a broadband all-textile slotted PIFA," *IEEE Trans. Antennas Propag.*, vol. 60, no. 1, pp. 379-384, Jan. 2012.

[11] C.- H. Lin, K. Saito, M . Takahashi and K. Ito, "A compact planar inverted-F antenna for 2.45 GHz on-body communications," *IEEE Trans. Antennas Propag.*, vol. 60, no. 9, pp. 4422-4426, Sep. 2012.

[12] Bluetooth low energy regulatory aspects, bluetooth SIG regulatory committee, V10r00, 2011.

[13] First Report and Order in the matter of revision of Part 15 of the Commission's rules regarding ultrawideband transmission systems, Federal Communications Commission, ET-Docket 98-153, 2002.

[14] T. Tuovinen, M. Berg, E. Salonen, "The effect of antenna pattern and polarization for launching creeping waves on a skin surface", in Proc. 8th Europ. Conf. Antennas Propag. (EuCAP), Apr. 2014, Hague, Netherlands, pp. 1960-1963.

[15] T. Tuovinen, M. Berg, W. G. Whittow and E. Salonen, "Performance of WBAN on-ground antenna type with relation to analytical path loss model", in Proc. 10th Loughborough Antennas Propag. Conf. (LAPC), Nov. 2014, Loughborough, United Kingdom, pp. 1-5.

[16] R. Paknys and N. Wang, "Creeping wave propagation constants and modal impedance for a dielectric coated cylinder," *IEEE Trans. Antennas Propag.*, vol. 34, no. 5, pp. 674-680, May. 1986.

[17] J. Puskely, M. Pokorny, J. Lacik and Z. Raida, "Antenna implementable into button for on-body communications at 61 GHz," in Proc. 8th Europ. Conf. Antennas Propag. (EuCAP), Apr. 2014, Hague, Netherlands, pp. 1739-1743.

[18] M. Berg, T. Tuovinen and E. Salonen, "Low profile antenna with optimal polarization for 2.45 GHz on-body sensor nodes", in Proc. 10th Loughborough Antennas Propag. Conf. (LAPC), Nov. 2014, Loughborough, United Kingdom, pp. 1-5.